Journal of Solid Mechanics Vol. 11, No. 4 (2019) pp. 902-917
DOI: 10.22034/jsm.2019.668662

Temperature Effect on Mechanical Properties of Top Neck Mollusk Shells Nano-Composite by Molecular Dynamics Simulations and Nano-Indentation Experiments

A. Nouroozi Masir [1], A. Darvizeh[1,*], A. Zajkani [2]

[1]*Department of Mechanical Engineering, University of Guilan, Rasht, Iran*
[2]*Department of Mechanical Engineering, Faculty of Engineering, Imam Khomeini International University, Qazvin, Iran*

Received 6 August 2019; accepted 11 October 2019

ABSTRACT

Discovering the mechanical properties of biological composite structures at the Nano-scale is much interesting today. Top Neck mollusk shells are amongst biomaterials Nano-Composite that their layered structures are composed of organic and inorganic materials. Since the Nano indentation process is known as an efficient method to determine mechanical properties like elastic modulus and hardness in small-scale, so, due to some limitation of considering all peripheral parameters; particular simulations of temperature effect on the atomic scale are considerable. The present paper provides a molecular dynamics approach for modeling the Nano-Indentation mechanism with three types of pyramids, cubic and spherical indenters at different temperatures of 173, 273, 300 and 373*K*. Based on load-indentation depth diagrams and Oliver-Far equations, the findings of the study indicate that results in the weakening bond among the bilateral atoms lead to reduced corresponding harnesses. Whenever, the temperature increases the elastic modulus decrease as well as the related hardness. Moreover, within determining the elastic modulus and hardness, the results obtained from the spherical indenter will have the better consistency with experimental data. This study can be regarded as a novel benchmark study for further researches which tend to consider structural responses of the various Bio-inspired Nano-Composites.

Keywords: Molecular dynamics simulation; Nano indentation; Nano-Composite; Top Neck mollusk shells; Temperature.

1 INTRODUCTION

NEW findings in the technology and science cause more than ever attention of scientists toward biomaterials and Nano-science. Regarding that Nano is a science that is capable to be present in different researches, therefore, several studies are reported here: Goodarzi et. al. [1-2-3], studied the effect of pretest on the vibrational frequency of rectangular Nano-sheets, and Nanotubes, respectively. Arda et. al. [4] studied the effect of vibrations on the Nanotubes and the effect of magnetic field on the carbon Nanotubes, Safarabadi et. al. [5] and Moradi et. al.

*Corresponding author.
E-mail address: adarvizeh@guilan.ac.ir (A.Darvizeh).

[6] studied the effect of vibrations on the Nano-beams, Nano-sheets, Zargaripoor et. al. [7] and Kordani et. al. [8] respectively Analyzed the vibrations of Nano-plastics made of FGM materials and piezoelectric Nanowires., Ghorbanpoor Aran et. al. [9-10-11], the studies on special polymers, carbon Nanotubes Piezoelectric layers and on the other hand Büşra Uzun [12] studied the free vibration analysis of BNNT with different cross-sections, Husseini [13], studied the effect of size on the Nanostructures, Asemi et. al.[14] and Mohammadi et. al.[15], studied the monolayer grapheme sheet.

Biological creatures are amongst the materials in the nature that have various types of structures in the Nano and micro scale. The structure of most batteries in the small scale is a multilayer Nano-Composite that causes marvelous mechanical and physical properties [16], [17], [18]. Mollusks are multilayer Nano-Composites with irregular and intricate structure, although this complicated structure is a simpler structure compared to other biological structures [19], [20]. Mollusks have diverse types and species that are classified into seven groups of: 1) Column structure, 2) Planar structure, 3) Horny structure, 4) Prismatic structure, 5) Layered structure, 6) Multiplex layered structure, 7) Homogeneous structure [21] (Fig.1).

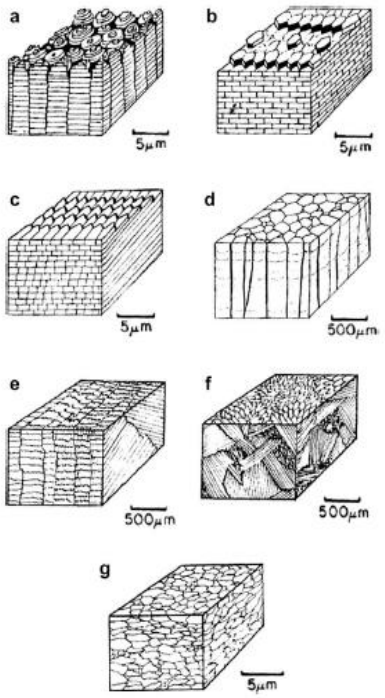

Fig.1
The structures forming sea shells, a) Column structure, b) Planar structure, c) Horny structure, d) Prismatic structure, e) Layered structure, f) Multiplex layered structure, g) Homogeneous structure.

The constituent structure of mollusks is a combination of organic and inorganic materials, and the inorganic materials are organized in the organic substrate [22], [23]. Flexibility is one of the mechanical properties which is inversely related to the strength of materials, but due to the special structure of biomaterials, these two factors are found together in the biomaterials such that in case of encountering the external forces, they can both show flexibility and strength to confront it. This is exclusive propoerty of biomaterials. Mollusks are among sea biomaterials that are no exception to this feature. They are one of the biomaterials that their crust function is basically mechanical and provides the protection of the biomaterial inside the shell and acts like a shield. The reason for this unique feature of biomaterial engineering structure including mollusks is that biological creatures can produce compounds in which organic and inorganic components lie together or are combined together in their complicated structure for survival [24], [25], [26]. The mollusk shell is an irregular Nano-Composite structure that is composed of inorganic (Aragonite) and organic (Chitin + Glycine) materials together in hierarchical layers [27] (Fig. 2).

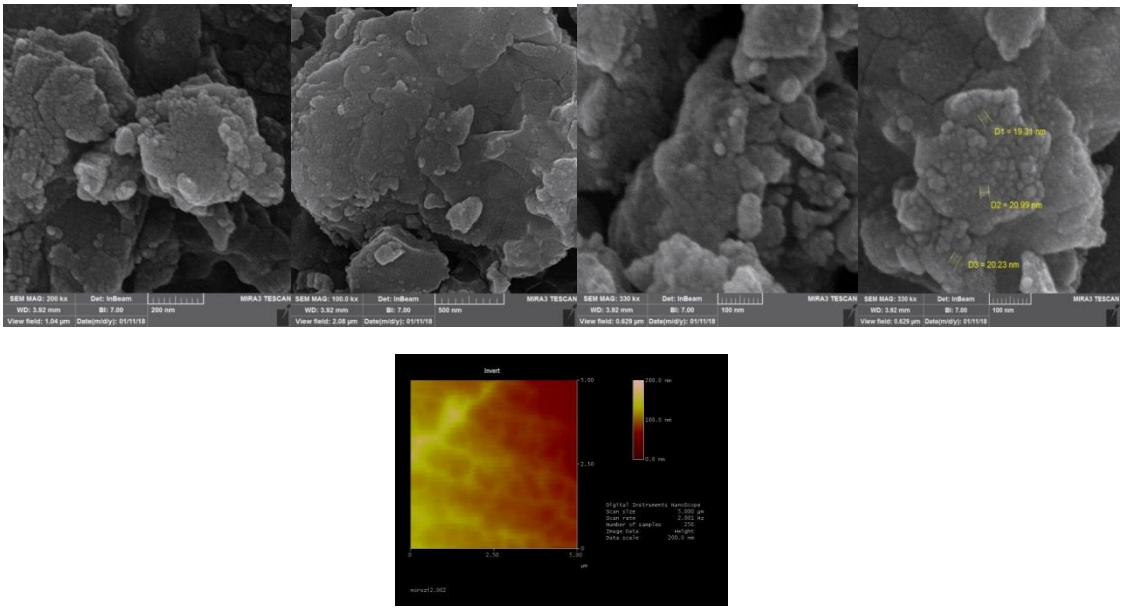

Fig.2
SEM-FE images of Top Neck mollusk shells in different scales.

The main constituent of this structure is Aragonite, which forms the maximum weight percentage of the biomaterial [28]. Together with organic materials, it forms Nano-layered composite [29], This issue caused the researchers to study the mechanical properties of this biomaterial and they are inspired by this for the structure of engineering materials [30] (Fig.3).

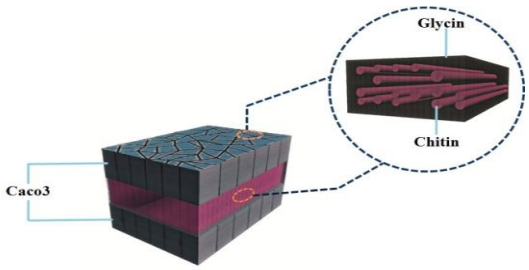

Fig.3
Hierarchical structure of mollusk .

There have been many studies on engineering and biomaterials in order to determine their mechanical characterization investigating microstructure properties using experimental Nano-indentation methods: [31], [29], [27], [32], [33], [34], [35], [18], [36] and [37]. It is obvious that most of them carried out in past decade are concerning about microstructure and mechanical properties of two types of mollusks; Conch and Abalone.

So, the main focus of this paper is on the mechanical characterization of another type of mollusks i.e. Top Neck mollusk shells. Due to non-destructive nature of the Nano-indentation, the method is known as a popular method and is widely used. But, in spite of the great advantages, the method has some limitations too. Therefore, due to significant sensitivity of indenter tip and experimental test apparatus, the effects of some parameters such as temperature, humidity and et al on the mechanical properties of the sample couldn't be performed. Therefore, nowadays, the numerical methods are used in the atomic scale to investigate the effect of these parameters [36], [22]. Although the molecular dynamic method has its limitations, including finding a suitable potential function for the interactions between atoms and the time-consuming modeling, and Nano-indentation experiment by molecular dynamic. Resolving this limitation needs the computers with very high capability. Regarding the recent technology advancements, the modeling is possible and the conditions which cannot be testes with the experimental methods are conducted with this method.

Today, development of MD simulations in various engineering sciences has become popular. Among the works developed for the Nano-indentation mechanism, although, some reports have been introduced by Sachin Patodia [38], Kizler and Schmauder et. al. [39], Peng et. al. [40], Ciccotti [41], Rocha and Hilbig [42], Fang [43] and Chao

pang [44]. But, there are no studies on the biomaterials including mollusks. Of courses, we can mention some studies of Yu and Lau [45], Zhang et. al. [36], Patodia et. al. [38], Jin et. al. [46] were done on the basis of the organic protein materials as the same of our work.

Accordingly, simulations of MD method have various capabilities and yet there has been no available the atomic- scale effort to characterizing the hardness and elastic modulus of the Top Neck mollusk Nano-Composite shells. Here, authors intend to investigate the problem by means of two different methods; the MD simulations and experimental considerations of the Nano indentation process.

2 NANO INDENTATION TESTING

2.1 Materials

All biological samples that are studied here are topneck mollusks shell collected from Persian Gulf, as shown in Fig. 4.

(a) (b)

Fig.4
a) The interior view of oysters. b) The exterior view of oysters.

2.2 Sample preparation

In order to reduce the error in the tests, the preparation method of the topneck mollusks shell for different conditions was same. For this, firstly, the shell has been prepared, and then a section with the dimensions of $1.0 \times 5.0 \times 1$ *mm* were prepared using a diamond knife and then inserted in a mold filled with resin (1 *cm* in diameter). For tightening, the samples were molded for 18 hours at room temperature in order to cure the resin (Fig. 5).

(a) (b)

Fig.5
Sample preparation for nano-indentation test. a) Sample cutting, b) Fixed sample inside resin.

Then, the samples were polished with emery paper to make the surface completely polished. In order to avoid any scratches on the surface, the samples were polished with different emery papers and finally, the surface quality degree was controlled using an optical microscope. To ensure that there are no scratches on the sample surface, after completion of the preparation stage, the samples were delivered to the laboratory for Nano-indentation tests.

2.3 Nano indentation Test

Nano-indentation is a very valuable and useful method to characterize the mechanical properties of material in the Nano scale. It is developed in the past two decades. It has made it possible to analyze and determine the mechanical properties like elastic modulus, hardness, creep behavior, and fracture toughness of materials. Piezoelectric based Newtonian electromagnetic forces in the scale of micron and Nano are applied on the surface of the material and the diagram of applied force variation versus indentation depth (hereafter called “depth”) is drawn. Elastic modulus and hardness are typical mechanical properties measured during indentation process, and both of these parameters could be calculated as a function of depth [47]. Since Nano-indentation test is considered as a non-destructive test, it is widely used by researchers and it’s fairly popular. The indenter is the principal component of the indentation system,

which has different geometries, shown in Fig.2. But, the most common type of the indenters is a Berkovich pyramidal indenter (Fig. 6(d) and Table 1).

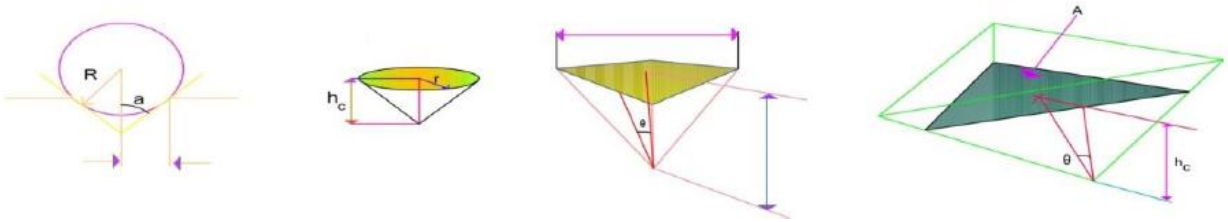

(a) (b) (c) (d)

Fig.6
Different types of indenters, a) Spherical, b) Pyramidal, c) Conical, d) Berkovich.

Table 1
The Berkovich Nano indenter properties. [55]

Thermal expansion	Thermal conductivity	Young's modulus (E)	Density	Mohs Hardness	Material
0.8	2050	1050	3.51	10	Diamond
$10^{-6}/C$	W($m\,k$)	*Gpa*	*g/cc*	Mohs-scale	

The results of the indentation test are used in order to obtain the elastic modulus and load-indentation depth graphs (Fig. 6). The tests covers the recording of the force versus indentation depth during loading from zero to maximum indentation and again from maximum load to the zero point.

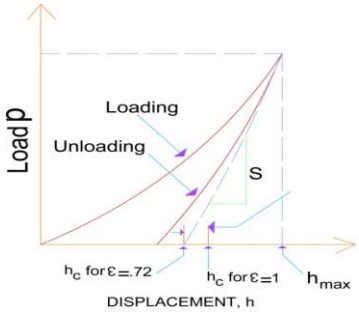

Fig.7
Force-depth diagram in nano indentation test.

The diagram in the Fig. 7 shows the maximum values of load and indentation depth. Moreover, mechanical properties like elastic modulus and hardness are obtained by measuring the slope of the diagram in the loading area (S). Eq. (1) is used in order to obtain the hardness.

$$H = \frac{F_{\max}}{A_c} \tag{1}$$

$F_{\max}$ and A are the sample's hardness, maximum indentation load and real contact area, respectively. Eq. (2) is used to calculate A_c, which is associated to the projection area in the distance from the indenter tip [11]. (Fig. 7)

$$A_c = C_0 h_c^2 + C_0 h_c + C_0 h_c^{\frac{1}{2}} + C_0 h_c^{\frac{1}{4}} \tag{2}$$

This equation usually fits with experimental data with good consistency (in a wide range of contact depths, as far as empirical data are taken on the reference sample surface). For any indenter, the C_1, C_2 and C_3 parameters in Eq. (2), are geometric parameters of the indenter tip [48]; so this could be obtained as Table 2.

Table 2
The relationship between the contact area and indentation depth for different indenters.

Indenter	Contact Area
Berkovich	$3\sqrt{3}h_c^2\tan^2(65.27)=24.5h_c^2$
Vickers	$4h^2\tan^2(68)=24.5h^2$
Knoop	$2h_c^2\tan 86.25\tan 65=65.43h_c^2$
Cube Corner	$3\sqrt{3}h_c^2\tan^2(35.26)=2.6h_c^2$
Spherical Corner	$62.83h_c^2$

h_c is the elastic deflection of the surface at a particular contact perimeter and it depends on the indenter geometry [47], therefore it could be obtained as:

$$h_c = h_{\max} - h_s \tag{3}$$

Therefore, h_s is calculated by the following equation.

$$h_c = \varepsilon\left(\frac{f_{\max}}{S}\right) \tag{4}$$

In this equation, ε is the indenter geometry contact; S is the curve slope of the load-indentation depth diagram under loading (Fig. 7) [47]. The real contact area is obtained using Eqs. (2)-(4), hardness of the sample is also obtained by insertion of the data from Table 1., in the Eq.(1). Finally, Eq. (5) is used to obtain the elastic modulus

$$E_r = \frac{1-v^2}{E} + \frac{1-v_i^2}{E_i} \tag{5}$$

E_s and E_i are Young modulus of the sample and the indenter, respectively, v_s and v_i are the Poisson ratio for the sample and indenter, respectively. As the indenter is not completely rigid, during the unloading some deformation occurs. It's therefore called the reduced elastic modulus and is calculated using the following equation:

$$E_r = \left(\frac{\sqrt{\pi}}{2B}\right)\left(\frac{s}{\sqrt{A_c}}\right) \tag{6}$$

where, B is the geometric constant of the indenter's tip[47], Whose values for the cubic and pyramidal indenter are 1,034 and for spherical indenter 1. E_s (Elastic modulus of the sample) is obtained with the Poisson's coefficient of the indenter (v_i), the elastic modulus of the indenter (E_i), the Poisson's coefficient of the sample (v_s), and the reduced elastic modulus (E_r) using Eq. (6).

3 MOLECULAR DYNAMIC SIMULATION

Molecular Dynamic simulation is very popular due to its capability in the Nano-indentation simulation atomic phase transformation [49], [22]. Molecular dynamics simulation is a numerical method from Newtonian movement equations for a set of atoms [49], [42], [50]. In this paper, The Top Neck mollusk shells Nano-Composite was simulated using PACKMOl software and Nano-indentation process was coded in LAMMPS (2018 version) and the Visual Molecular Dynamics (VMD) and Open Visualization Tools (OVITO) were used for visualization. In this simulation, the indenters were diamonds that were applied on the surface of the bio-Nano-Composites. The atoms used for the construction of used indenters (Fig. 8), were carbon with atomic number of 12 that the number of its

atoms for construction of the indenters with different geometries and their complete information is shown in Table 3.

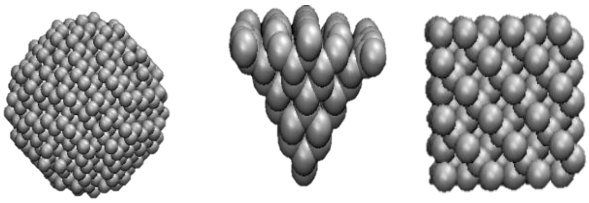

(a) (b) (c)

Fig.8
Different indenters' simulation: a) Spherical indenter, b) Pyramidal indenter, c) Cubic indenter.

Table 3
The simulated indenters' specifications.

	Material	Atomic number	No of Atom	Radius	Districts	Radius of base
Spherical indenter	Diamond	12	19840	2.5	-----	-----
Cubic indenter	Diamond	12	26400	-----	5*5	-----
Pyramidal indenter	Diamond	12	11795	-----	-----	2.5

The sample in this simulation process is a bio Nano-composite that its dimensions in the *X, Y* and *Z* directions are 160, 180 and 160 *Å*, respectively (Fig. 9).

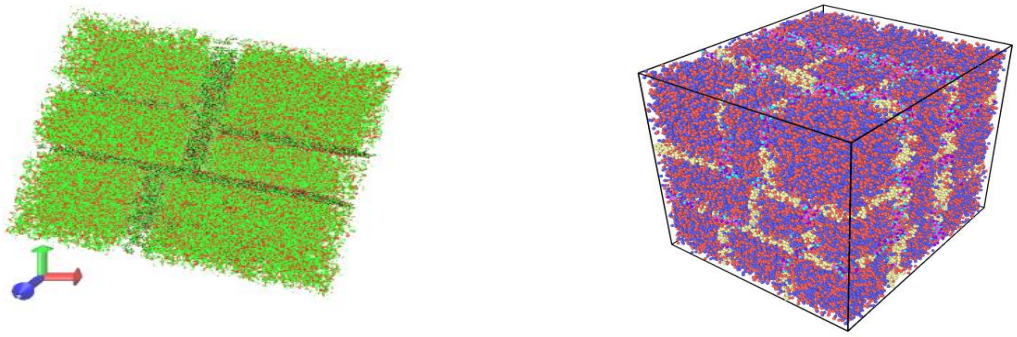

Fig.9
Molecular dynamics simulation of the bio nano-composite.

As it is shown in the Fig. 9, the bio Nano-Composite has an irregular structure and organic materials (Chitin-Glycine) are between Aragonite blocks. In this simulated structure, there are 314502 atoms used that from these number, Aragonite has 191802 atoms and Glycine has 44135 atoms and Chitin has 78565 atoms. All the atoms used in this structure are five types of *H, C, N, Ca, O*. The temperatures used in this process are 173, 273, 300 and 373*K* and the movement equations are integrated using Verlet algorithm [51] with time steps of 1×10^{-14} *s*. the variables in the Nano-indentation process are listed in Table 4., and the main parameters for process coding are shown in Table 5.

Table 4
The MD simulation parameters.

	Dimensions	Number of atoms
Bio Nano-Composite	160*180*160	314502
Spherical indenter	sphere radius of 2.5 *nm*	19840
Pyramidal indenter	Sharp tip with a radius of 2.5 *nm*	11795
Cubic indenter	Size of the sides is 5 *nm*	26400
Distance between the indenter and sample	0	0
Maximum Depth	5.025	5.025

Table 5
The fundamental parameters for nano-indentation simulation coding.

	Description
Sample material	Diamond
Indentation Type	Controlled displacement *t* the intended depth
Balance temperature	300 *K*
Indentation rate	50 MS^{-1}
Time Step	1×10^{-14}
Boundary condition	Periodic
Maximum indentation depth	5.025 *nm*

According to this, for the starting the Nano-indentation processes, at first, the indenters are in contact with the topneck mollusks shell Nano-Composite (Fig. 10).

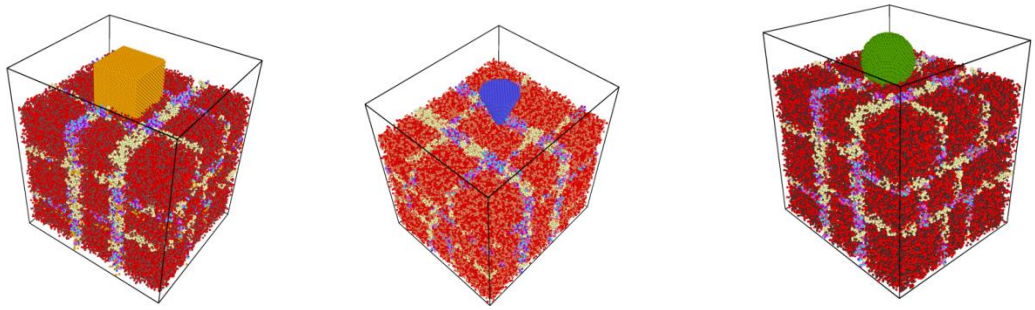

(a) (b) (c)

Fig.10
Nano-indentation process simulation on the Top Neck mollusk shells with different indenters. a) Cubic indenter, b) Pyramidal indenter, c) Spherical indenter.

The next step is the selection of a force field for consideration of interactions between atoms in molecular dynamics simulation and it is an important step to express the potential function. So that for a molecular system with *N* particles the following equation will be obtained:

$$U\left(r_1, r_2, ...r_N\right) = \sum_i Q_1\left(r_i\right) + \sum_{i,j \succ i} Q_2\left(r_i, r_j\right) + \sum_{i,j \succ i,k \succ j} Q_3\left(r_i, r_j, r_k\right) + ... \tag{7}$$

In this equation, *r* is the atom center location vector, Q_1 represents the external field effect, Q_2 is the interaction of molecular pair and Q_3 is the interaction between three particles. In this paper, Dreiding potential function was used to calculate the mutual forces between *H, C, N, Ca* and *O* atoms. This potential function has four principal terms as follows:

1) bond stretching term
2) changes in bond angle term
3) changes in dihedral rotation term
4) van der Waals non-bonded interactions term

According to this, the general form of Dreiding potential function is as follows:

$$E_{total} = E_{bond}\left(r\right) + E_{angle}\left(\theta\right) + E_{dihedral}\left(\varphi\right) + E_{non-bonfing}\left(r\right) \tag{8}$$

In Eq.(8), the terms $E_{bond}\left(r\right)$, $E_{angle}\left(r\right)$, $E_{dihedral}\left(r\right)$ and $E_{non-bonfing}\left(r\right)$ are calculated via Eqs. (9), (10), (11) and (13).

$$E_{bond}\left(r\right) = \frac{1}{2} k_b \left(r - r_e\right)^2 \tag{9}$$

$$E_{bond}(\theta)=\frac{1}{2}k_{\theta}(\theta-\theta_e)^2 \tag{10}$$

$$E_{bond}(\varphi)=\sum_{i=1}^{3}C_i(\cos\varphi)^i \tag{11}$$

where θ_e and r_e are the equilibrium bond angle and bond length, k_θ and k_b are stiffness constants for the bond angle potentials and bond length potentials, respectively. On the other hand, the k_b in each band is 700 $K\ cal/mol/A^2$ and depending on the number of the atoms that form the angle and based on the number of the angles, the value of $K_{ij}(n)=nK_{ij}(1)$ will be obtained so that for n = 1, n = 2, n= 3 the value of k_θ will be obtained as $700\,K\ cal/mol/A^2$, 1400 $K\ cal/mol/A^2$ and 2100 $K\ cal/mol/A^2$ and C_i represents the coefficients of dihedral multi-harmonic and C_i represents the coefficients of dihedral multi-harmonic. The C_i value is calculated with the following equation that is dependent on the effect of indenter rupture on the atoms and C_i represents the coefficients of dihedral multi-harmonic. The value of C_i is calculated from the following equation, which depends on the effect of the collapse failure on the atoms.

$$C_{ij}=\frac{K_{ij}}{\left(\sin\theta_j^0\right)^2} \tag{12}$$

which the value of C_{ij} is obtained by having the value K_{ij} and θ_j^0. On the other hand, the value of $E_{non-bonfing}(r)$ is obtained from the following equation.

$$E_{non-bonfing}(r)=4\varepsilon\left[\left(\frac{\sigma}{r}\right)^{12}-\left(\frac{\sigma}{r}\right)^{6}\right],r\prec r_c \tag{13}$$

where r is the distance between two atoms, σ is the distance at zero energy, ε is the energy well depth and r_c is the cutoff distances that taken as 10.5 $\AA$. In particular for this study, the value of each constant for Top Neck mollusk shells Nano composite is presented in the following Table 6.

Table 6
Basic parameters for the dreiding potential function.

Atom	$(A^0)\,r_e$	$(\deg)\,\theta_e$	σ
H	0.330	180	12.382
C	0.770	109.471	14.23
N	0.702	106.7	13.843
O	0.660	120	13.843
Ca	1.94	90	12
Cl	0.994	180	13.861
Na	1.86	90	12

Also, in this process, for balancing the system, a NVT thermostat and following a NVE thermostat for temperature control in various temperatures are used.

4 RESULTS AND DISCUSSION

In the loading and unloading time, indenter penetrates in the sample and causes the destruction of the sample. As shown in Fig. 11, the indentation extent for different indenters in various times is different.

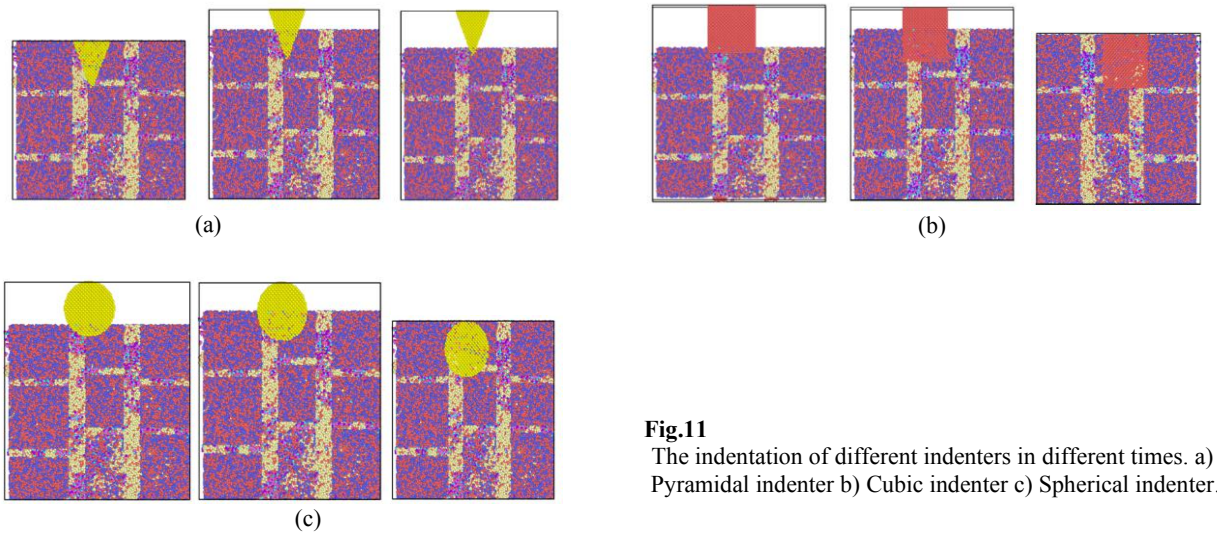

Fig.11
The indentation of different indenters in different times. a) Pyramidal indenter b) Cubic indenter c) Spherical indenter.

The output of the loading and unloading of the indentation process is load-indentation depth. Fig. 12 shows the load-indentation depth diagram resulted from Nano-indentation process using spherical, cubic and pyramidal indenters on the Top Neck mollusk shells Nano-Composite in the temperatures of 173, 273, 300 and 373 *K* for various indenters.

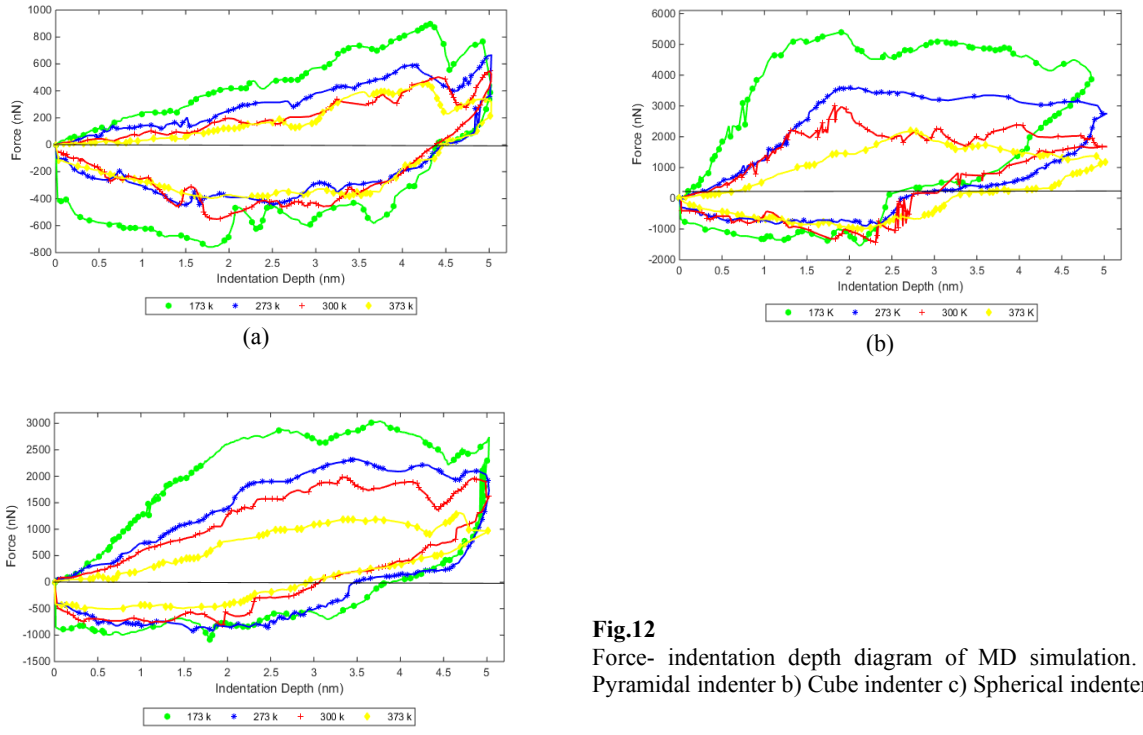

Fig.12
Force- indentation depth diagram of MD simulation. a) Pyramidal indenter b) Cube indenter c) Spherical indenter.

As it is shown in the Fig. 12, in the equal maximum indentation depth, the required force for reaching this displacement for various types of indenters in different temperatures are different. With information like maximum load, indentation depth and information about the sample and indenter, the elastic modulus can be obtained, which for this the slope of the diagram during unloading must be calculated. The needed information like $h_{\max}, F_{\max}, S, v, v_i, E_i, E$ and ε are shown in Table 7.

Table 7
Effective parameters for calculating the mechanical properties in MD simulation .

MD Information Types of indenter	temperature	h_{max} (nM)	h_c (nM)	A_p (nM^2)	S (mN/nM)	h_f (nM)	h_f / h_{max}
Spherical Indenter	173	5.025	4.74995	354.224	1385.214	3.7994	0.7561
	273	5.025	5.33622	447.062	1865.012	3.4438	0.685333
	300	5.025	4.31517	292.345	1987.658	3.0487	0.606706
	373	5.025	5.38587	455.419	2037.548	2.9167	0.580438
Cube Indenter	173	5.025	-0.5293	0.728511	521.35	2.4404	0.485652
	273	5.025	-0.5009	0.65247	373	2.6080	0.519005
	300	5.025	0.39782	0.41147	232	2.6415	0.525672
	373	5.025	0.35469	0.327101	188.1	4.46428	0.888414
Berkovich Indenter	173	5.025	4.75654	554.079	2235	4.4136	0.878328
	273	5.025	4.79772	563.715	1980	4.4851	0.892557
	300	5.025	4.81835	568.574	1900	4.363046	0.868268
	373	5.025	4.88082	583.410	1648.89	4.44945	0.885463

By using the data in Table 7., and Eqs. (1-6) the elastic modulus of the Top Neck mollusk shells Nano-Composite will be determined that with other outputs of the molecular dynamics simulation shown in Table 8.

Table 8
Elastic modulus obtained using various indenters.

Mechanical Properties	Berkovich Indenter				Cube Indenter				Spherical Indenter			
	173	273	300	373	173	273	300	373	173	273	300	373
E	0.033	0.0327	0.033	0.032	0.911706	0.963418	1.21348	1.361209	79.933	92.184	99.239	93.695
H	1.443	1.064	0.920	0.543	5299.86	4212.053	4076.737	3580.893	7.0715	3.8596	6.4348	2.1662

In the following, the results of the Nano-indentation test for comparison with the obtained results were analyzed. In this way, after sample preparation, for the Nano-indentation test, the diamond indenter (Berkovich type) with loading and unloading rate of 20 *mN/MIN* and the load of 10 *mN* is applied on the sample surface. Nano-indentation on the sample, as shown in Fig. 13, was applied on five points that for every indent, there would be an indentation effect and a load-indentation depth will be obtained.

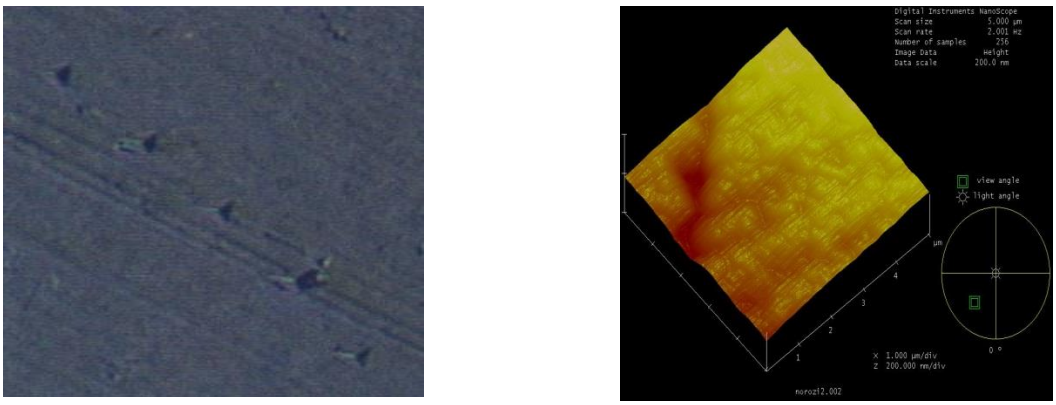

Fig.13
Effect of indenter on the sample.

Therefore, to analyze this process, five different graphs of load versus indentation depth like Fig. 14 must be plotted.

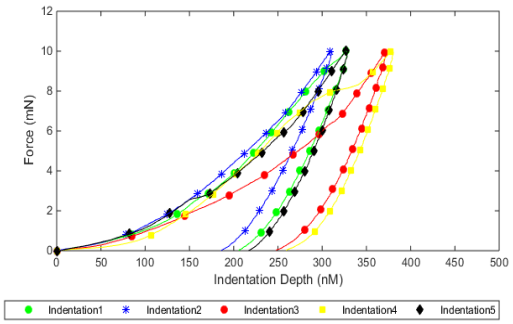

Fig.14
Force- indentation depth diagram of Top Neck mollusk shells.

Loading and unloading type in the experimental test linearly increased from zero to 100 μN, and then in the unloading, the load decreased from 100 μN to zero (Fig. 15). The extracted parameters from Fig. 14 are shown in the Table 9.

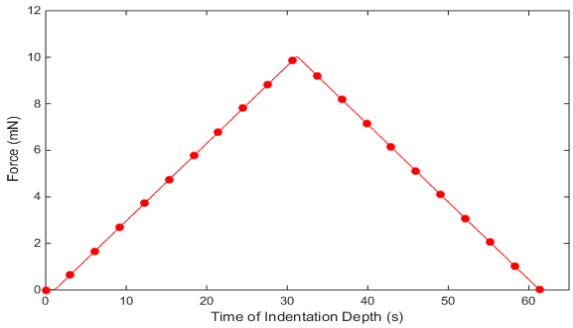

Fig.15
Force-time diagram at loading and unloading stage.

Table 9
Effective parameters in calculation of mechanical properties.

Test information Types of shell	NO. Indetation	h_{max} (nM)	h_c (nM)	h_p (nM)	A_p (nM^2)	S (mN/nM)	Hardness	Elastic Modulus
Top Neck mollusk shells	Indent1	327.77	269.02	208.53	1966143.38	0.1279	5106.076	83.807
	Indent2	310.20	248.30	189.33	1695788.13	0.1222	5922.873	86.394
	Indent3	372.38	320.55	252.36	2731472.00	0.1431	3678.219	79.248
	Indent4	379.06	328.19	264.47	2856375.50	0.1460	3518.470	79.032
	Indent5	327.68	275.00	220.31	2048058.75	0.1425	4901.107	92.069

To calculate the mechanical properties of each sample like elastic modulus and hardness, in general, the mean elastic modulus and the obtained hardness should be calculated and these calculated parameters should be considered as the mechanical properties of the samples. Finally, using the data in Table 9., and Eq.(1) to Eq.(6), the elastic modulus (Fig. 16) and hardness (Fig.17) will be calculated.

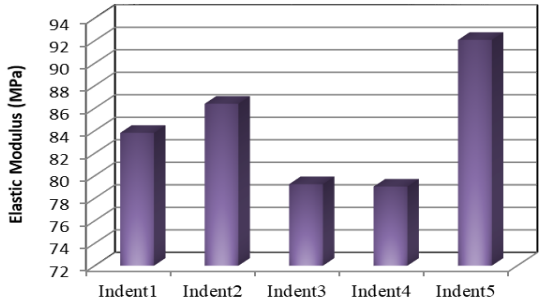

Fig.16
Total elastic modulus of Top Neck mollusk shells sample with MD.

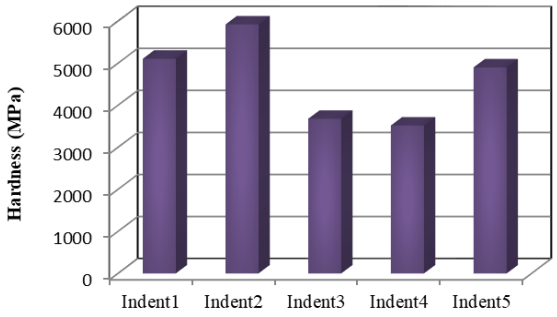

Fig.17
Total hardness of Top Neck mollusk shells sample with MD.

Table 10
Mechanical propertied from experimental method and MD simulation.

	Indenter Types	*H* (*GPa*)	*E* (*GPA*)
Experimental Test	Berkovich Indenter	4625.749	84.11

According to this, the elastic modulus and hardness of Top Neck mollusk shells using experimental Nano-indentation method will be calculated as 4625.749 *MPa* and 84.110*GPa*. In order to validate the experimental tests and molecular dynamics, it is necessary to justify some deficiencies in the molcular dynamics simulation. One of the deficiencies in the MD process is that the time and calculation source has made the conditions difficult for validation of molecular dynaimc simulation with experimental tests so that it has confided the longitudinal scales to some Nanometer or thousands or millions of aroms. Moreover, the rate used in molecular dynamic simulation versus the experimental rate is a factor that may cause unreal or unwanted effects on the output results. Therefore, it might be predicted that the rate change in the Nano-indentation process can make strain rate variation. In this paper, in order to study the effect of loading, some experiments using molecular dynamics at various rates of 10 *m/s*, 50 *m/s*, 100 *m/s* and 150 *m/s* were carried out.

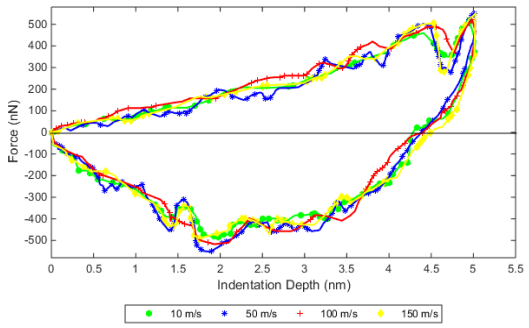

(a)

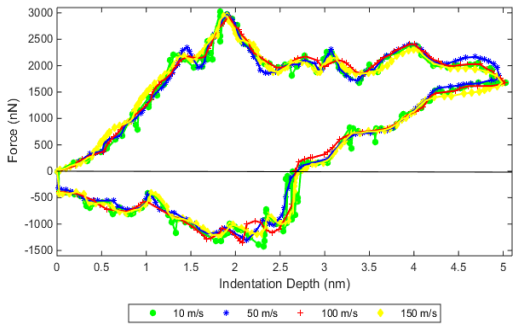

(b)

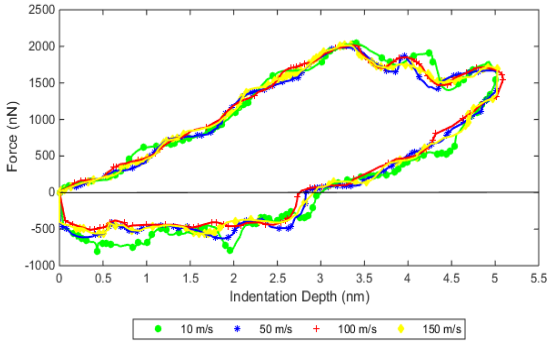

(c)

Fig.18
Load-indentation depth diagram at various rates: a) Cubic, b) Pyramidal, c) Spherical.

In order to validate the experimental tests and molecular dynamics, it's necessary to justify some deficiencies in the molcular dynamics simulation.

As it's seen from Fig. 18, the loading rate doesn't have much effect on the load-indentation depth diagram. These results are consistent with Naihara [52] obervations, that he claimed that large hydrostatic parts effect (penetration in Nano-indentation process) can cause plastic deformation in any material. Never the less, Table 8., and Table 10., demonstrate comparing mechanical propertie of Top Neck mollusk shells obtained from two different methods of molecular dynamics simulation and experimental test method.

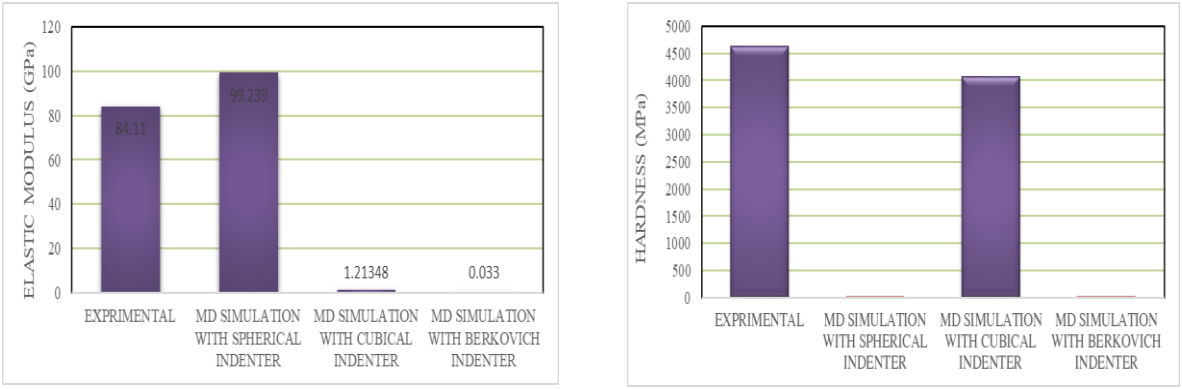

(a) (b)

Fig.19
Comparison of the mechanical properties obtained using two different indenters, a) Elastic modulus b) Hardness.

As shown in Fig. 19, when using spherical indenter in molecular dynamic simulation, the elastic modulus and hardness will be 99239 *MPa*, 6.4348, for pyramidal indenter, the elastic modulus and hardness will be 0.033 *MPa* and 0.92 *GPa*, for cubic indenter, the elastic modulus and hardness will be 1.21348 *MPa* and 4076.737 *GPa* and the results from experimental Nano-indentation test presents the elastic modulus and hardness of 4635.749 *MPa* and 84.110 *GPa*.

Therefore, it is well understood that Nano-indentation simulation using molecular dynamics method gives helpful information about various types of indenters. However, as shown in Table 4., about the spherical indenter tip, it is not comparable with experimental tests. On the other hand, in the experimental Nano-indentation test, because of the Berkovich indenter with some Nanometer tip (not being sharp in the Nano scale), it could be considered as spherical indenter. The difference is that the indenter with sharp tip will cause shear stress in the sample but the spherical indenter causes elastic stress in the sample. This is because that in the equal indentation depth, the energy needed for deformation of the Top Neck mollusk shells Nano-Composite in spherical indenter is higher than pyramidal (conical) indenter.

Generally, it could be deduced that the results of the molecular dynamic simulation using spherical and cubic indenters for determination of elastic modulus and hardness are in good consistency with the results obtained from experimental indentation using the Berkovich indenter, and there is good consistency between the molecular dynamics simulation and experimental tests.

5 CONCLUSIONS

In the present paper, mechanical properties such as elastic modulus and hardness of topneck mollusks shell Nano composite were studied by using molecular dynamics simulation in different temperatures with three indenters. The mechanical properties were determined by using load-indentation depth diagrams and Oliver-Far equations. To validate the mechanical properties of various indenters, the results of the molecular dynamics in the temperature of 300*K* were compared to the experimental results. The results show that the hardness obtained using cubic indenter, and the elastic modulus obtained using spherical indenter by MD method, have good consistency with experimental results. Accordingly, for the temperature effect, the results show that as the temperature increases the elastic modulus and hardness of the sample decrease. This is consistent with the previous work [53][54] that states with the increase of the temperature, the hardness and elastic modulus decrease.

REFERENCES

[1] Goodarzi M., Mohammadi M., Farajpour A., Khooran M., 2014, Investigation of the effect of pre-stressed on vibration frequency of rectangular Nanoplate based on a visco-Pasternak foundation, *Journal of Solid Mechanics* **6**(1): 98-121.

[2] Tavaf V., Bahrami M.N., Goodarzi M., 2017, Refined plate theory for free vibration analysis of FG Nanoplates using the nonlocal continuum plate model, *Journal of Computational Applied Mechanics* **48**(1): 123-136.

[3] Goodarzi M., Mohammadi M., Khooran M., Saadi F., 2016, Thermo-mechanical vibration analysis of FG circular and annular Nanoplate based on the visco-pasternak foundation, *Journal of Solid Mechanics* **8**(4): 788-805.

[4] Arda M., Aydogdu M., 2018, Longitudinal magnetic field effect on torsional vibration of carbon nanotubes, *Journal of Computational Applied Mechanics* **49**(2): 304-313.

[5] Safarabadi M., Mohammadi M., Farajpour A., Goodarzi M., 2013, Effect of surface energy on the vibration analysis of rotating nanobeam, *Journal of Solid Mechanics* **7**(3): 299-311.

[6] Moradi A., Ghanbarzadeh A., Jalalvand M.,Yaghootian A., 2018, Magneto-thermo mechanical vibration analysis of FG nanoplate embedded on visco pasternak foundation, *Journal of Computational Applied Mechanics* **49**(2): 395-407.

[7] Daneshmehr A., Zargaripoor A., Rajabpoor A., Isaac-Hosseini I., 2018, Free vibration analysis of nanoplates made of functionally graded materials based on nonlocal elasticity theory using finite element method,*Journal of Computational Applied Mechanics* **49**(1): 86-101.

[8] Kordani N., Farajpour A., Divsalar M., Fereidoon A., 2016, Forced vibration of piezoelectric Nanowires based on nonlocal elasticity theory, *Journal of Computational Applied Mechanics* **47**(2): 137-150.

[9] Ghorbanpour Arani A., Haghparast E., Baba Akbar Zarei H., 2016, Application of halpin-tsai method in modelling and size-dependent vibration analysis of CNTs/fiber/polymer composite microplates, *Journal of Computational Applied Mechanics* **47**(1): 45-52.

[10] Ghorbanpour Arani A., Amir S., Karamali Ravandia A., 2015, Nonlinear flow-induced flutter instability of double CNTs using reddy beam theory, *Journal of Computational Applied Mechanics* **46**(1): 1-12.

[11] Ghorbanpour Arani A., Fereidoon A.,Kolahchi R., 2014, Nonlocal DQM for a nonlinear buckling analysis of DLGSs integrated with Zno piezoelectric layers, *Journal of Computational Applied Mechanics* **45**(1): 9-22.

[12] UzunB., Numanoglu H., Civalek O., 2018, Free vibration analysis of BNNT with different cross-sections via nonlocal FEM, *Journal of Computational Applied Mechanics* **49**(2): 252-260.

[13] Hosseini M., Hadi A., Malekshahi A., Shishesaz M., 2018, A review of size-dependent elasticity for nanostructures, *Journal of Computational Applied Mechanics* **49**(1): 197-211.

[14] Asemi S.R., Mohammadi M., Farajpour A., 2014, A study on the nonlinear stability of orthotropic single-layered graphene sheet based on nonlocal elasticity theory, *Latin American Journal of Solids and Structures* **11**(9): 1515-1540.

[15] Mohammadi M., Farajpour A., Goodarzi M., Mohammadi H., 2013, Temperature effect on vibration analysis of annular graphene sheet embedded on visco-Pasternak foundation, *Journal of Solid Mechanics* **5**(3): 305-323.

[16] Jin Me S., Wan Lin G., 2010, Chmical- mechanical stablity of the hierarchical structure of mshell nacre, *Science China Physics, Mechanics and Astronomy* **53**(2): 380-388.

[17] Lv J., Jiang Y., Zhang D., 2015, Structural and mechanical characterization of atrina pectinata and freshwater mussel shells, *Journal of Bionic Engineering* **12**(2): 276-284.

[18] Addadi L., Joester D., Nudelman F., Weiner S., 2006, Mollusk shell formation: A source of new concepts for understanding biomineralization processes, *Chemistry* **12**(4): 980-987.

[19] Sarikaya M., Gunnison K.E., Yasrebi M., Aksay I.A., 1990, Mechanical property–microstructural relationship in abalone shell, *Symposium R – Materials Synthesis Utilizing Biological Processes* **174**: 325-452.

[20] DeVol R.T., Sun C.Y., Marcus M.A., Coppersmith S.N., Myneni S.C., Gilbert P.U., 2015, Nanoscale transforming mineral phases in fresh nacre, *Journal of the American Chemical Society* **137**(41): 13325-13333.

[21] Horacio D.E., Jee E.R., Barthelat F., Markus J.B., 2009, Merger of structure and material in nacre and bone - perspective on de novo biomimetic material, *Progress in Materials Science* **54**: 1059-1100.

[22] Zhi-Hui X., Xiaodong Li, 2011, Deformation strengthening of biopolymer in nacre, *Advanced Functional Materials* **21**(20): 3883-3888.

[23] Horacio D., Jee E.R., Barthelat F., Buehler M. J., 2009, Merger of structure and material in nacre and bone - Perspectives on de novo biomimetic materials, *Progress in Materials Science* **54**(8): 1059-1100.

[24] Bruet B.J.F., Qi H.J., Boyce M.C., Panas R., Tai K., Frick L., Ortiz C., 2005, Nanoscale morphology and indentation of individual nacre tablets from the gatropod mollusc trochus niloticus, *Journal of Materials Research* 20(9): 2400-2419.

[25] Meguid S. A., Alian A. R., 2018, *Micromechanics and Nanomechanics of Composite Solids,* Springer.

[26] Barthelat F., Horacio D., Jee E.R., 2003, Elastic properties of nacre aragonite tablets, *Journal of Applied Mechanics* **68**: 2-7.

[27] Furuhashi T., Schwarzinger C., Miksik I., Smrz M., Beran A., 2009, Molluscan shell evolution with review of shell calcification hypothesis, *Comparative Biochemistry and Physiology Part B* **154**(3): 351-371.

[28] Rodrigues J. R., Alves N. M., Mano J. F., 2017, Nacre-inspired Nano-Composites produced using layer-by-layer assembly: Design strategies and biomedical applications, *Materials Science and Engineering C* **76**: 1263-1273.

[29] Weiss I. M., Tuross N., Addadi L., Weiner S., 2002, Mollusc larval shell formation: Amorphous calcium carbonate is a precursor phase for aragonite, *Journal of Experimental Zoology* **293**(5): 478-491.

[30] Finnemore A., Cunha P., Shean T., Vignolini S., Guldin S., Oyen M., Steiner U., 2012, Biomimetic layer-by-layer assembly of artificial nacre, *Nature Communications* **3**: 966.
[31] Li X., Chang W.-C., Chao Y. J., Wang R., Chang M., 2004, Nanoscale structural and mechanical characterization of a natural Nano-Composite material: the shell of red abalone, *Nano Letters* **4**(4): 613-617.
[32] Lee Y. H., Islam S.M., Hong S.J., Cho K.M., Math R.K., Heo J.Y., Kim H., Yun H.D., 2010, Composted oyster shell as lime fertilizer is more effective than fresh oyster shell, *Biosci Biotechnol Biochem* 74(8): 1517-1521.
[33] Kunitake M.E., Mangano L.M., Peloquin J.M., Baker S.P., Estroff L.A., 2013, Evaluation of strengthening mechanisms in calcite single crystals from mollusk shells, *Acta Biomater* **9**(2): 5353-5359.
[34] Cowin S. C., Hegedus D.H., 1976, Bone remodeling II: theory of adaptive elasticity, *Journal of Elasticity* **6**(3): 313-326.
[35] Sumitomo T., Kakisawa H., Owaki Y., Kagawa Y., 2007, Structure of natural nano-laminar composites: TEM observation of nacre, *Materials Science Forum* **561-565**: 713-716.
[36] Zhang N., Yang S., Xiong L., Hong Y., Chen Y., 2016, Nanoscale toughening mechanism of nacre tablet, *Journal of the Mechanical Behavior of Biomedical Materials* **53**: 200-209.
[37] Lee S. W., Kim Y. M., Kim R. H., Choi C. S., 2008, Nano-structured biogenic calcite: A thermal and chemical approach to folia in oyster shell, *Micron* **39**(4): 380-386.
[38] Patodia S., Bagaria A., Chopra D., 2014, Molecular dynamics simulation of proteins: A brief overview, *Journal of Physical Chemistry & Biophysics* **4**(6): 166-175.
[39] Kizler P., Schmauder S., 2007, Simulation of the nanoin- dentation of hard metal carbide layer systems—the case of nanostructured ultra-hard carbide layer sys- tems, *Computational Materials Science* **39**: 205-213.
[40] Peng P., Liao G., Shi T., Tang Z., Gao Y., 2010, Molecular dynamic simulations of nanoindentation in aluminum thin film on silicon substrate, *Applied Surface Science* **256**(21): 6284-6290.
[41] Ciccotti G., 2009, Molecular dynamics simulation, *Journal of Micro/Nanolithography, MEMS, and MOEMS* **8**(2): 21151-21158.
[42] Rocha J. R., Yang K. Z., Hilbig T., Brostow W., Simoes R., 2013, Polymer indentation with mesoscopic molecular dynamics, *Journal of Materials Research* **28**(21): 3043-3052.
[43] Fang T. H., Wu J. H., 2008, Molecular dynamics simulations on Nanoindentation mechanisms of multilayered films, *Computational Materials Science* **43**(4): 785-790.
[44] Peng C., Zeng F., 2017, A molecular simulation study to the deformation Behaviors and the size effect of polyethylene during Nanoindentation, *Computational Materials Science* **137**: 225-232.
[45] Yu Z., Lau D., 2015, Molecular dynamics study on stiffness and ductility in chitin–protein composite, *Journal of Materials Science* **50**(21):7149-7157.
[46] Jin K., Feng X., Xu Z., 2013, Mechanical properties of chitin-protein interfaces: A molecular dynamics study, *BioNanoscience* **3**(3): 312-320.
[47] Pharr G.M., Oliver W.C., Brotzen F.R., 1999, On the generality of the relationship among contact stiffness, contact area, and elastic modulus during indentation, *Journal of Materials Research* **7**: 613-617.
[48] Oliver W.C., Pharr G.M., 1992, An improved technique for determination hardness and elastic modulus using load and displacment sensing indentation exprimental, *Journal of Materials Research* **7**: 1564-1583.
[49] Ning Zhang Y.C., 2013, Nanoscale plastic deformation mechanism in single crystal aragonite, *Journal of Materials Science* **48**: 785-796.
[50] Terrell E.J., Landry E., Mcgaughey A., Iii C.F.H., 2017, *Molecular Dynamics Simulation of Nano Indentation.*
[51] Goel S., Haque Faisal N., Luo X., Yan J., Agrawal A., 2014, Nanoindentation of polysilicon and single crystal silicon: Molecular dynamics simulation and experimental validation, *Journal of Physics D: Applied Physics* **47**(27): 275304.
[52] Niihara K., 1979, Slip system and olastic deformation of silicon carbid single crystal at hightemperatures, *Journal of the Less Common Metals* **65**: 155-166.
[53] Wang H., Hu M., Xia M., Ke F., Bai Y., 2008, Molecular/cluster statistical thermodynamics methods to simulate quasi-static deformations at finite temperature, *International Journal of Solids and Structures* **45**(13): 3918-3933.
[54] Amaya-Roncancio S., Arias-Mateus D.F., Gómez-Hermida M.M., Riaño-Rojas J.C., Restrepo-Parra E., 2012, Molecular dynamics simulations of the temperature effect in the hardness on Cr and CrN films, Applied Surface Science **258**(10): 473-4477.
[55] Zaremba C. M., 1996, Critical transitions in the biofabrication of abalone shells and flat pearls, *Chemistry of Materials* **8**(3): 679-690.